27th ABCM International Congress of Mechanical Engineering
December 04-08, 2023, Florianópolis-SC, Brazil

COB-2023-0936
EXPERIMENTAL INVESTIGATION AND NUMERICAL SIMULATION OF HEAT TRANSFER AND PRESSURE DROP OF MWCNT/THERMAL OIL NANOFLUID FLOWING INSIDE A HORIZONTAL TUBE

Daniel Alberto Flórez Morales
Edwin Martin Cardenas Contreras
Erick Oliveira do Nascimento
Enio Pedone Bandarra Filho
Federal University of Uberlandia, Mechanical School. Uberlandia (MG), Brazil. Av. Joao Naves de Ávila, 2121.
esdanielflorez@gmail.com
emcardenas.1989@gmail.com
erick.nascimento@ufu.br
bandarra@ufu.br

Abstract. *This work presents an experimental and numerical simulation performed to evaluate the thermohydraulic performance of multi-walled carbon nanotubes (MWCNT) nanoparticles dispersed in thermal oil, flowing in a horizontal tube under constant heat flux conditions. The goal is to investigate the effect of adding MWCNT nanoparticles to the thermal oil on heat transfer and pressure drop. Nanofluids with volumetric concentrations of 0.01% and 0.02% were produced using the sonication process. The experimental setup evaluated the heat transfer coefficient and pressure drop in laminar flow, with an inlet temperature of 60 °C, mass flow rate of 17 g/s, and constant heat flux conditions on the tube surface of 12 kW/m². For numerical simulation, the same experimental test conditions were considered. The finite volume method implemented in Ansys Fluent software was used, assuming single-phase, Newtonian, and incompressible flow. The experimental results showed that the dispersion of carbon nanotubes increased the heat transfer coefficient compared to the base fluid, while the pressure drop was higher. Numerical simulations exhibited satisfactory agreement with experimental data. The analysis of the results indicates that the addition of MWCNT nanoparticles in thermal oil can significantly improve heat transfer and pressure drop. This study contributes to understanding of the nanoparticle effects on thermal fluids and can contribute to the development of systems with improved heat transfer performance.*

Keywords: *Carbon Nanotubes, Heat transfer, Nanofluids, Numerical Simulation, Pressure Drop*

1. INTRODUCTION

Heat transfer fluids such as water, ethylene glycol and oil are used in many fields of applications, but they have poor heat transfer properties compared with most solids. How to improve their thermophysical properties is one of the greatest challenges to their application. Therefore, many researchers have focused their efforts on the development of high-performance heat transfer fluids in recent decades. So, advancement in nanotechnology gives an opportunity to disperse nanoparticles (1-100 nm) in based liquid, which is called nanofluids by Choi (1995). In fact, it was found that nanofluids have improved thermophysical properties when compared to baseline fluids, thereby demonstrating a great potential for application in thermal systems (Asadi et al., 2018).

There is a limited number of experimental works on heat transfer from nanofluids with oil as the base fluid. These works are mainly studied within a laminar flow, which may be due to the high viscosity of these fluids. Several studies on heat transfer and pressure drop of oil-based nanofluids can be found in the literature. Saeedinia et al. (2012) experimentally investigated the average heat transfer coefficient of CuO/MO nanofluids flowing inside a horizontal tube under constant heat flux. The findings indicated an increase in the average heat transfer coefficient with increasing concentration of carbon nanotubes. The maximum increase in the heat transfer coefficient was 12.7 % for a concentration of 2 wt.%. Kumaresan et al. (2013), for instance, mentioned an enhancement of 150 % and 92 % of the heat transfer coefficient at x/D=93.46 for MWCNT/H_2O-EG nanofluids (70:30), whose nanoparticle volumetric concentrations were 0.450 % and 0.150 %. The authors attributed the significant enhancement in the convective heat transfer to the migration of carbon nanotubes within the base fluid, which disrupts the rapid development of the thermal boundary layer. Hekmatipour et al. (2016) analyzed the convection heat transfer in thermal oil-based CuO nanofluids in a laminar flow. The researchers showed an increase in the heat transfer coefficient with the increase in the concentration of nanoparticles. The observed increments were in the order of 22 % for a nanoparticle concentration of 1.5 wt.%. Detailed literature reviews on the heat transfer behavior of nanofluids were provided by Yu et al. (2008) and Murshed et al. (2011). Amiri et al. (2015) experimentally assessed the convection heat transfer of carbon nanotube nanofluids in turbine oil flowing inside a horizontal circular tube in laminar flow ($Re : 350 - 750$). The authors prepared stable nanofluids at different concentrations (0.001 %, 0.010 %, 0.050 % and 0.100 vol.%). According to the findings, as the solid concentration of carbon nanotubes increased, the convection heat transfer coefficient increased in all axial positions along the tube.

In literature, several experimental and numerical works can be found aiming to evaluate convective heat transfer in nanofluids. However, it is important to highlight that few studies have focused on the use of thermal oil as the base fluid. Regarding the numerical approach, single-phase and two-phase models are the most commonly used. The single-phase approach assumes that the fluid and particles move at the same velocity. This approach has lower computational demand and has been employed in various studies on convective heat transfer with nanofluids ((Sajjad et al., 2018), (Liang et al., 2019), (Saeed et al., 2021) and (Bose at al., 2023)). On the other hand, the two-phase approach takes into account factors such as gravity, Brownian forces, turbulence, among others. However, this approach is more complex and requires higher computational cost for implementation.

In this work, convective heat transfer and pressure drop were evaluated in laminar flow of carbon nanotube (MWCNT) nanofluids dispersed in thermal oil. Volumetric concentrations of 0.01% and 0.02% were experimentally tested in a horizontal tube with constant heat flux on the wall. In addition, numerical solutions were obtained by solving the Navier-Stokes and energy equations using the ANSYS Fluent software based on the finite volume method, assuming single-phase flow due to the very low concentration. In the study, the mass flow rate was kept constant at 17 g/s, and a constant heat flux of 12 kW/m^2 was applied to the external surface of the tube wall. The inlet temperature of the tested samples into the tube was maintained at 60 °C. The effect of nanoparticle concentration on the convective heat transfer coefficient and pressure loss was experimentally evaluated and compared with the base fluid. The results of the numerical/experimental comparison were presented as variations of the Nusselt number (Nu) and convective heat transfer coefficient (h) along the tube, as well as variations in the outlet temperature (T_{out}) values and friction factor (f).

2. METHODS

2.1 Materials

The present study used multiwalled carbon nanotubes with a length range of 30-40 µm and a diameter range of 20-30 nm for the production of nanofluids. These nanotubes were obtained from Nanostructures & Amorphous Material Inc. The baseline fluid employed in this research was LUBRAX-OT100 mineral oil, which was provided by PETROBRAS. Detailed information regarding their thermophysical properties of the nanoparticles and base fluid can be found in Table 1.

Table 1. Thermophysical properties of nanoparticles and base fluid.

Properties	**Base fluid***	**MWCNT**
Thermal Conductivity [W/m·K]	0.131	3000
Specific Heat [J/kg·K]	1883	710
Density [kg/m^3]	885	2100
Dynamic Viscosity [Pa·s]	0.31	-

* The thermophysical properties of the base fluid were demonstrated at a temperature of 20 °C.

To calculate the properties of the nanofluids, the models introduced by Pak and Cho (1998) (Eq. (1)) and Xuan and Rotzel (2000) (Eq. (2)) were employed.

$$\rho_{nf} = (1 - \emptyset)\rho_{bf} + \emptyset\rho_{np} \tag{1}$$

$$C_{p,nf} = \frac{(1 - \emptyset)\rho_{bf}C_{p,bf} + \emptyset\rho_{np}C_{p,np}}{(1 - \emptyset)\rho_{bf} + \emptyset\rho_{np}} \tag{2}$$

2.2 Preparation of nanofluids

The two-step method is used for the production of oil-based carbon nanotube nanofluids at different concentrations (0.01 and 0.02 vol.%) (Saeedinia et al., 2012). Due to the high viscosity of the thermal oil, the turbine agitator is first used to facilitate the dispersion of particles within the base fluid for 15 minutes. Once the mechanical agitation process is completed, the samples are submitted to an ultrasonic bath-type process, for which a low-power ultrasonic bath (50 W) was used for 2 hours. In this process, the breaking of the aggregates and the dispersion of particles homogeneously is observed. Subsequently, each sample is sonicated using a programmable ultrasonic processor, applying a power of 400 W with a frequency of 20 kHz with pulses in ON of 5 s and time in OFF of 8 s for 2 hours. The ultrasonic processor generates heat during operation because all the energy is dispersed in the fluid, causing an increase in fluid temperature. Then, a cooling water bath is used to dissipate heat from the nanofluids during ultrasonic homogenization. The temperature of the nanofluids during the process remained constant. Finally, a complete dispersion of the nanoparticles in the base oil is observed.

2.2 Experimental setup

The experimental setup has the necessary features to study the thermal and fluid dynamic behavior of the oil-based carbon nanotube nanofluids produced. The experimental apparatus used for this case is illustrated schematically in Figure 1. It consists of a test section, the cooling system, the preheating system, and mass flow measurement system, and the monitoring system and data acquisition.

The test section designed to determine the convective heat transfer coefficient and pressure drop of nanofluids in laminar flow with constant surface heat flux, consists of a brass circular tube with smooth inner wall, an external diameter of 12.7 mm, wall thickness of 3.17 mm and a total length of 2480 mm. To measure wall temperatures, the test section has 8 T-type thermocouples and 8 PT100-type RTD temperature sensors, distributed at 8 points along the outer wall of the tube. It is worth noting that each of the 8 points contains a thermocouple and a PT100 in diametrically opposite positions. Thus, the temperature measuring instruments are fixed in grooves made in the tube in different positions, starting from the inlet.

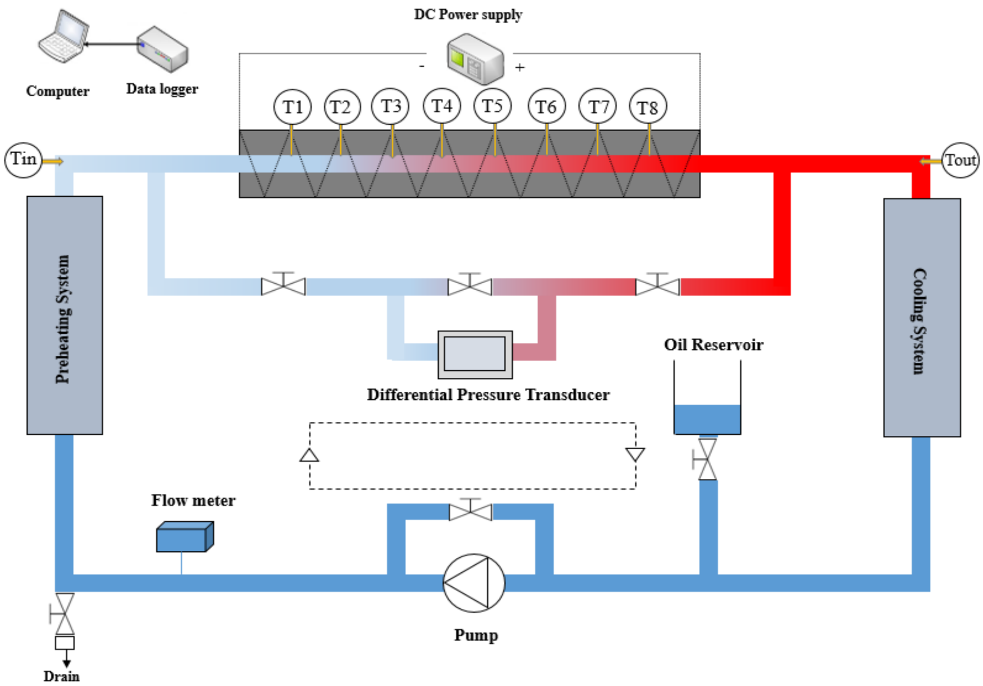

Figure 1. Schematic diagram of the experimental bench.

The equipment responsible for maintaining the fluid flow in the main circuit is a gear pump, which was installed on the experimental setup, proving to be appropriate in the operating conditions performed. Two air vent valves were placed at the highest locations to eliminate or minimize the presence of bubbles in the flow. The Coriolis flowmeter is responsible for measuring the mass flow and consists of a sensor transmitter assembly. The Coriolis type sensor (model RHM06-4F1PS) and the transmitter or electronic unit (model CMM01) were supplied by METROVAL Ltda.

The constant heat flux boundary condition applied to the tube wall was obtained by the heating of 12 flexible tape-type electrical resistances insulated with polyamide, model KH (supplied by OMEGA ENGINEERING, INC). These flexible tapes are fixed over the entire external area of the test section tube with a polyamide adhesive tape. The electrical power required for heating the resistive tapes was controlled by a voltage regulator.

To evaluate the pressure, drop and friction factor of nanofluids, two piezoresistive pressure transmitters PSI40 ZURICH were installed to measure the gauge pressure at the inlet and outlet of the test section. Further, a differential pressure transmitter LD301 ESMAR with simultaneous recording of data was installed to obtain the pressure drop more accurately.

2.3 Numerical approach

The refrigerant fluids analyzed numerically in this work are considered single-phase, incompressible, and Newtonian, with constant properties, as performed by Sadri et al. (2018) and Liang et al. (2019). Based on these considerations, the mass, momentum, and energy conservation equations, as given by (3-5), implemented in the Ansys Fluent (Fluent, 2013).

$$\frac{\partial(u_i)}{\partial x_i} = 0 \tag{3}$$

$$\rho u_i \frac{\partial u_j}{\partial x_i} = -\frac{\partial p}{\partial x_i} + \frac{\partial}{\partial x_i}\left[\mu\left(\frac{\partial u_j}{\partial x_i}\right)\right] \tag{4}$$

$$\rho C_p\left(u_i \frac{\partial T}{\partial x_i}\right) = k\left(\frac{\partial^2 T}{\partial x_i^2}\right) \tag{5}$$

where ρ, μ, C_p, and k refer to the density, dynamic viscosity, specific heat, and thermal conductivity of the refrigerant fluid, respectively. The variable p represents pressure, u_i is the component of the velocity vector, and x_j is the cartesian coordinate vector (Liang et al., 2019).

Similar to the experimental tests, the flow was considered to be in a laminar flow (Reynolds number 151 – 166) and hydrodynamically developed in the entrance region, with constant mass flow rate and temperature at 17 g/s and 60 °C, respectively, for volumetric concentration of 0.01 % and 0.02 %. At the outlet, a zero value was assumed for static pressure. The wall region was set with a no-slip condition.

The friction factor obtained experimentally in different Reynolds numbers was compared with the friction factor obtained through the theoretical model widely used in the literature for hydrodynamically developed laminar flow, described by Eq. (7). The experimental results of the friction factor were calculated through the pressure drop in the test section as shown in Eq. (8).

$$T_t = T_{in} + \frac{q'' \cdot \pi \cdot D \cdot z}{\dot{m} \cdot L} \tag{6}$$

$$f_t = \frac{64}{Re} \tag{7}$$

$$f = \frac{\pi^2 \cdot D^5 \cdot \rho \cdot \Delta p}{8\dot{m} \cdot L} \tag{8}$$

Eq. (9) is obtained, which defines the local convective heat transfer coefficient.

$$h(z) = \frac{q''}{T_s(z) - T_f(z)} \tag{9}$$

The average value of the convective heat transfer coefficient was obtained with the values of the local coefficient h(z) at the different measurement points using Eq. (10).

$$h_{avg} = \frac{h(x_1) + \cdots + h(x_n)}{n} \tag{10}$$

The local Nusselt number can be calculated using Eq. (11), while the average Nusselt number can be determined using Eq. (12).

$$Nu(z) = \frac{h(z) \cdot D}{k} \quad (11)$$

$$Nu_{avg} = \frac{Nu(z_1) + \cdots + Nu(z_n)}{n} \quad (12)$$

3. RESULTS

The Table 2 presents the mesh independence using the outlet temperature and the friction factor of the fluid, with comparison to experimental results and the Hagen-Poiseuille equation, to validate the numerically obtained results. Three unstructured meshes with different element sizes were used for this procedure, as performed by Sadri et al. (2018).

Table 2. Mesh independence and validation of numerical results.

Parameter\Mesh	**1**	**2**	**3**
Number of elements	436656	638024	868572
Temperature - CFD [ºC]	74,67	76,67	76,81
Difference – CFD&Experimental [%]	-7,38 %	4,90%	4,73%
Difference – CFD&Theoretical [%]	-3,08 %	0,49%	-0,31%
Friction Factor – CFD [-]	0,390	0,389	0,389
Difference – CFD&Experimental [%]	45,00 %	44,67 %	44,53 %
Difference – CFD&Theoretical [%]	1,01 %	0,78 %	0,79 %

As seen in Table 2, mesh 2 shows better results in terms of thermal and hydraulic performance. The outlet temperature of the tube with the mesh containing 638,024 elements exhibits a difference of only 0.49 % compared to the value obtained using Eq. (6). Compared to the experimental value, the difference was less than 5 %, and there was no significant change in its value with increasing mesh refinement. The friction factor diverges when compared to the experimental result, which can be attributed to the low Reynolds number and the uncertainty of the pressure measurement equipment. However, when compared to the Hagen-Poiseuille equation, there was only 0.77 % difference. Additional mesh refinement beyond mesh 2 did not generate significant variation in the results. Thus, Mesh 2 was selected for the simulation in this study.

As illustrated in Figure 2, the numerical model demonstrates satisfactory agreement with the experimentally obtained results using Eq. (6). It is noteworthy that the numerical model exhibits better agreement with the theoretical results. Additionally, a significant reduction in fluid temperature occurred experimentally with the addition of nanoparticles, despite the increase in thermal conductivity. However, it was numerically identified, and through Eq. (6), that the fluid outlet temperature increased with the increase in volumetric concentration of nanoparticles, indicating that the nanofluids show promising results in heat exchangers.

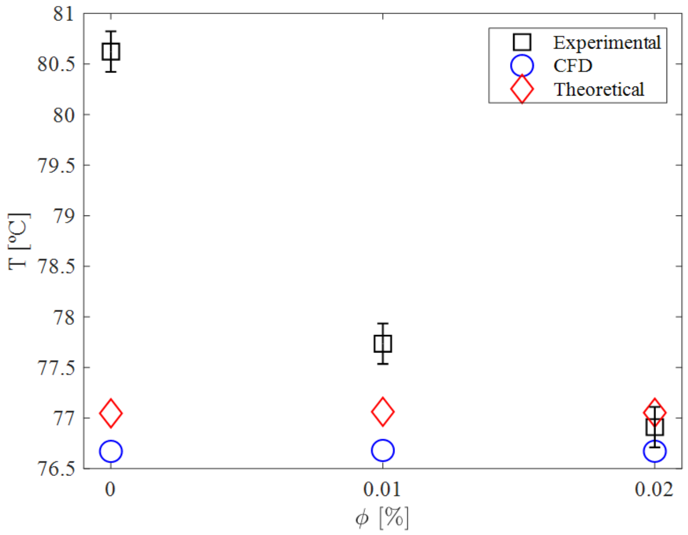

Figure 2. Fluid coolant outlet temperature in relation to nanoparticle concentration.

Figure 3 illustrates the local heat transfer coefficient as a function of axial distance. It was identified that the numerical results show satisfactory agreement compared to the experimental results, with an average difference of 3.12%, which is particularly for the region starting from 1.4 m, where the experimental results show an increase in the convective coefficient with axial distance, contrary to what was obtained in the numerical results. Additionally, a maximum increase of 0.05 % and 9.53 % in the local convective coefficient was identified for the nanofluids with volumetric concentration of 0.01 % and 0.02 %, respectively, at the position of 0.165 m, while experimentally, for the nanofluid with the lowest volumetric concentration, a reduction of up to 2.99 % and an increase of up to 7.90 % were observed.

As can be observed in Figure 4, as expected, the average numerical heat transfer coefficient shows agreement with the experimental results as well as the local values. The numerical results indicate that the nanofluids exhibits increased in the average convective heat transfer coefficient of 0.04 % and 8.09 % for volumetric concentration of 0.01 % and 0.02 %, respectively, compared to the base fluid, while experimentally, a reduction in the average convective coefficient of up to 1.83 % was observed for the nanofluid with the lowest nanoparticle concentration. However, for the nanofluid with a volumetric concentration of 0.02 %, an increase of up to 1.53 % was identified. Therefore, it can be stated that the analyzed nanofluids have a concentration of 0.01 vol. % showed gains within the measurement uncertainty range, while for the volumetric concentration of 0.02 %, promising numerical results were observed, indicating that nanofluids have the potential to improve stability and enhance heat transfer, mainly due to the fact that the numerically obtained values fall within the measurement uncertainty range.

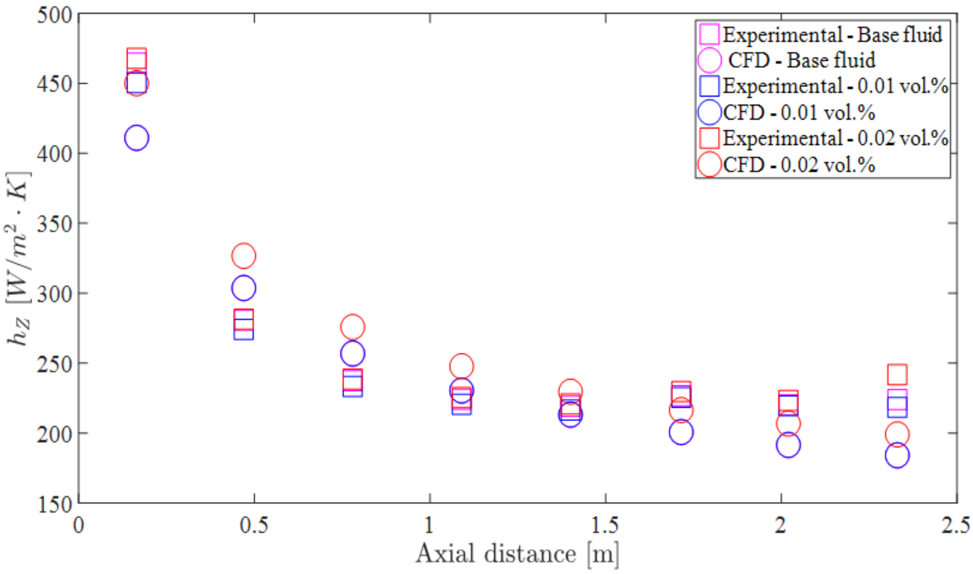

Figure 3. Local convective coefficient as a function of axial distance.

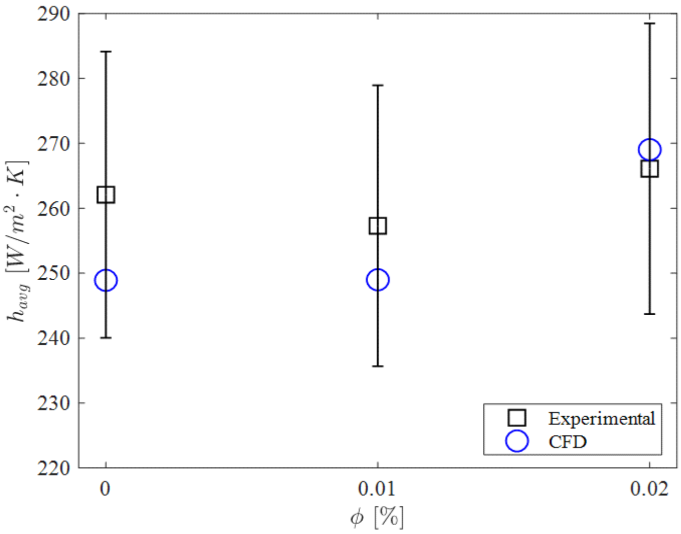

Figure 4. Average convective heat transfer coefficient as a function of nanoparticle concentration.

As observed in Figure 5, the numerical results demonstrate satisfactory agreement with the experimental results regarding the local Nusselt number. In the case of the base fluid, the average Nusselt number showed a difference of only 5.03 %, a value that can be attributed to the simplification made in the numerical model and the unexpected behavior of the local Nusselt number beyond the 1.4 m position, where it tends to increase with tube length. When comparing the local values with increasing nanoparticle concentration, both numerical and experimental analyses identified a reduction in the Nusselt number of up 0.05 % and 3.06 %, respectively, for the nanofluid with a volumetric concentration, both numerical simulation and experiments revealed an increase in the Nusselt number of up to 9.41 % and 25.98 %, respectively.

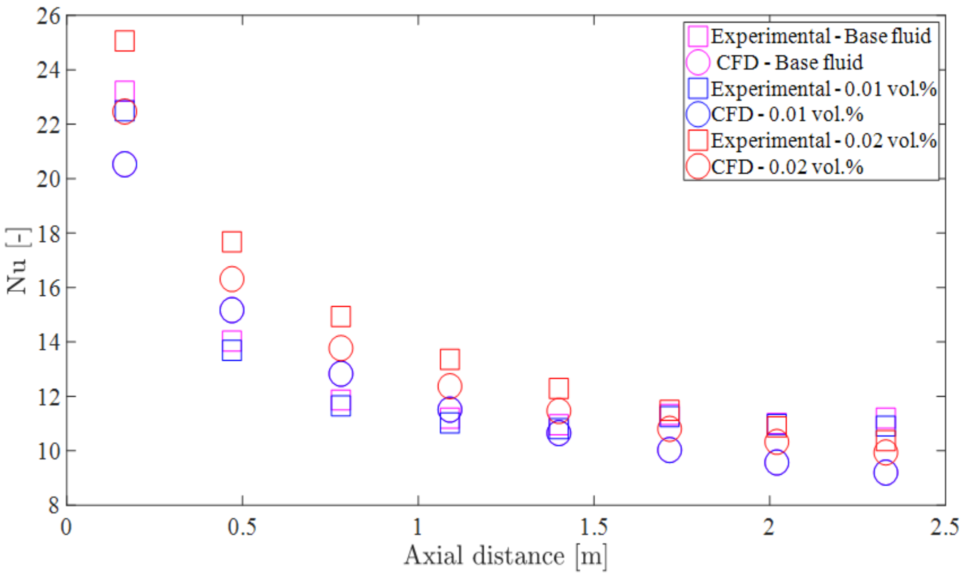

Figure 5. Nusselt number as a function of axial distance.

As observed in Figure 6, it was identified that numerically, the average Nusselt number shows a decrease of 0.04 %, while in the experiments, a reduction of 1.91 % was observed for the nanofluid with a volumetric concentration of 0.01 % compared to the base fluid. However, for the nanofluid with a concentration of 0.02 vol.%, an increase of up to 7.98 % and 10.74 % was observed through numerical and experimental analysis, respectively. Similarly, to the average convective heat transfer coefficient, the average Nusselt numbers obtained numerically fall within the measurement uncertainty range.

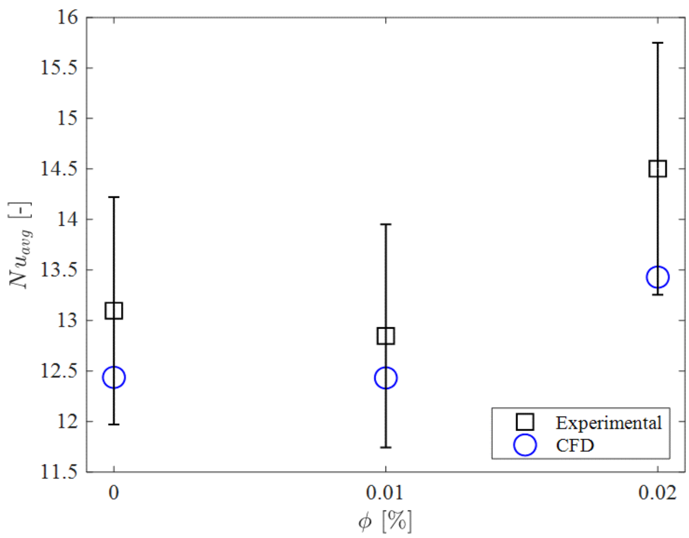

Figure 6. Average Nusselt number as a function of nanoparticle concentration.

Figure 7 illustrates the friction factor variation with respect to the concentration of MWCNT nanoparticles, obtained through experiments, numerical simulations, and the Hagen-Poiseuille equation. It was found that the numerical model exhibits satisfactory agreement with the theoretical model, with a maximum difference of only 0.78 %. Additionally, the addition of nanoparticles did not significantly affect the discrepancies between the numerical model and the Hagen-Poiseuille equation.

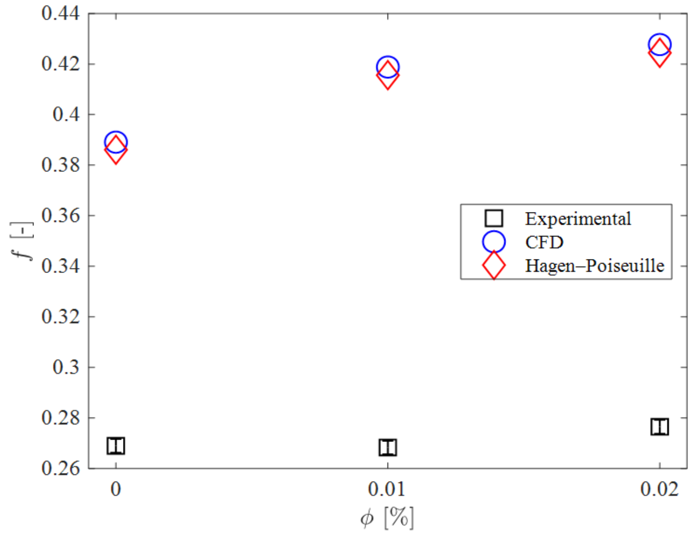

Figure 7. Friction factor as a function of nanoparticle concentration.

However, both the numerical and theoretical models deviated from the experimental results, showing an average difference of 51.83 %. This significant difference can be attributed to the experimental measurement uncertainty in pressure drop, which tends to have greater impact at low Reynolds number, as observed in the results of Sajjad et al. (2018). Furthermore, an increase in the friction factor of up to 2.80 %, 9.93 % and 9.91 % was identified in the experimental, numerical, and Hagen-Poiseuille equation results, respectively. It is worth noting that the numerical increases are directly proportional to the increment in dynamic viscosity caused by the increase in nanoparticle volumetric concentration.

4. CONCLUSIONS

This work investigates convective heat transfer and pressure drop in laminar flow inside a horizontal circular tube using MWCNT/thermal oil nanofluids. The study focuses on nanoparticle concentrations of 0.01% and 0.02%, a mass flow rate of 17 g/s, and a constant heat flux of 12 kW/m^2. Experimental and numerical analyses were performed to validate the results. Numerical results show that nanofluids exhibit a 0.04% increase in average convective heat transfer coefficient for a concentration of 0.01% and an 8.09% increase for a concentration of 0.02% compared to the base fluid. In contrast, experimental results indicate a reduction of up to 1.83% for the nanofluid with the lowest nanoparticle concentration. The average Nusselt number decreases by 0.04% numerically and by 1.91% experimentally for a concentration of 0.01% compared to the base fluid. However, for a concentration of 0.02%, numerical and experimental analyses reveal increases of 7.98% and 10.74%, respectively. Additionally, the friction factor increases by up to 2.80% experimentally, 9.93% numerically, and 9.91% according to the Hagen-Poiseuille equation, in line with the rise in dynamic viscosity caused by increased nanoparticle concentration. The study recommends using a two-phase model to predict the thermal and hydraulic behavior of carbon nanotube nanofluids and compare it with single-phase and experimental approaches. This approach provides a comprehensive understanding of the system characteristics.

5. ACKNOWLEDGEMENTS

The authors are grateful for the financial support provided for this research by CAPES, CNPq and FAPEMIG.

6. REFERENCES

Amiri, A., Shanbedi, M., Yarmand, H., Arzani, H. K., Gharehkhani, S., Montazer, E., Sadri, R., Sarsam, W., Chew, B. T., and Kazi, S. N., 2015. "Laminar convective heat transfer of hexylamine-treated MWCNTs-based turbine oil nanofluid". *Energy Conversion and Management*, v. 105, p. 355–367.

Asadi, A., Asadi, M., Rezaniakolaei, A., Rosendahl, L. A., and Wongwises, S., 2018. "An Experimental and Theoretical Investigation on Heat Transfer Capability of Mg (OH)2/MWCNT-Engine Oil Hybrid Nano-Lubricant Adopted as a Coolant and Lubricant Fluid". *Applied Thermal Engineering*, v. 129, p. 577-586.

Bose, J. R., Manova, S., Angeline, A. A., Asirvatham, L. G., and Gautam, S., 2023. "Numerical Study on the Heat Transfer Characteristics of Cu-Water and TiO2-Water Nanofluid in a Circular Horizontal Tube". *Energies*, v. 16, n. 3, p. 1449.

Choi, S. U. S., and Eastman, J. A., 1995. "Enhancing Thermal Conductivity of Fluids with Nanoparticles". *American Society of Mechanical Engineers, Fluids Engineering Division*, San Francisco (CA), USA.

Fluent, A. User's Guide. 2013. Ansys Fluent Theory Guide. ANSYS Inc., USA, v. 15317, p. 724-46.

Hekmatipour, F., Akhavan-Behabadi, M. A., Sajadi, B, 2016. "Combined free and forced convection heat transfer of the copper oxide-heat transfer oil (CuO-HTO) nanofluid inside horizontal tubes under constant wall temperature". *Applied Thermal Engineering*, v. 100, p. 621–627.

Kumaresan, V., Mohaideen Abdul Khader, S., Karthikeyan, S., and Velraj, R., 2013. "Convective heat transfer characteristics of CNT nanofluids in a tubular heat exchanger of various lengths for energy efficient cooling/heating system". *International Journal of Heat and Mass Transfer*, v. 60, n. 1, p. 413–421.

Liang, Y., Liu, P., Zheng, N., Shan, F., Liu, Z., Liu, W., 2019. Numerical investigation of heat transfer and flow characteristics of laminar flow in a tube with center-tapered wavy-tape insert. *Applied Thermal Engineering*, v. 148, p. 557-567.

Murshed, S. M. S., Nieto de Castro, C. A., Lourenço, M. J. V., Lopes, M. L. M., and Santos, F. J. V., 2011. "A Review of Boiling and Convective Heat Transfer with Nanofluids". *Renewable and Sustainable Energy Reviews*, v. 15, n. 5, p. 2342–2354.

Pak, B.C.; Cho, Y.I., 1998. "Hydrodynamic and heat transfer study of dispersed fluids with submicron metallic oxide particles". *Experimental Heat Transfer*, v. 11, n. 2, p. 151-170.

Sadri, R., Mallah, A.R., Hosseini, M., Ahmadi, G., Kazi, S.N., Dabbagh, A., Yeong, C.H., Ahmad, R., Yaakup, N.A, 2018. "CFD modeling of turbulent convection heat transfer of nanofluids containing green functionalized graphene nanoplatelets flowing in a horizontal tube: comparison with experimental data". *Journal of Molecular Liquids*, v. 269, p. 152-159.

Saeedinia, M., Akhavan-Behabadi, M. A., Razi, P., 2012. "Thermal and rheological characteristics of CuO-Base oil nanofluid flow inside a circular tube". *International Communications in Heat and Mass Transfer*, v. 39, p. 152–159.

Saeed, F. R., Jasim, M. A., Mahmood, N. B., and Jaffar, Z. M., 2021. "Numerical investigation of convective heat transfer of single wall carbon nanotube nanofluid laminar flow inside a circular tube". *Archives of Thermodynamics*, v. 42, n. n. 2, p. 103–119.

Sajjad, M., Kamran, M.S., Shaukat, R., Zeinelabdeen, M.I.M., 2018. Numerical investigation of laminar convective heat transfer of graphene oxide/ethylene glycol-water nanofluids in a horizontal tube. *Engineering Science and Technology, An International Journal*, v. 21, n. 4, p. 727-735.

Shah, R. K.; London, A. L., 1978. Advances in heat transfer. Laminar Forced Flow Convection in Ducts, Suppl, v. 1.

Yu, W., France, D.M., Routbort, J.L., Choi, S.U.S., 2008. "Review and comparison of nanofluid thermal conductivity and heat transfer enhancements". *Heat Transfer Engineering,* v. 29, n. 5, p. 432-460.

Xuan, Y.; Roetzel, W., 2000. "Conceptions for heat transfer correlation of nanofluids". *International Journal of Heat and Mass Transfer*, v. 43, n. 19, p. 3701-3707.

7. RESPONSIBILITY NOTICE

The authors are the only responsible for the printed material included in this paper.